

# Ionization Properties of Phosphatidylinositol Polyphosphates in Mixed Model Membranes<sup>†</sup>

Edgar E. Kooijman,<sup>‡</sup> Katrice E. King,<sup>§</sup> Mahinda Gangoda,<sup>§</sup> and Arne Gericke<sup>\*,§</sup>

<sup>‡</sup>Department of Biological Sciences and <sup>§</sup>Department of Chemistry, Kent State University, Kent, Ohio 44242

Received May 20, 2009; Revised Manuscript Received August 11, 2009

**ABSTRACT:** Phosphatidylinositol polyphosphate lipids (phosphoinositides) form only a minor pool of membrane phospholipids but are involved in many intracellular signaling processes, including membrane trafficking, cytoskeletal remodeling, and receptor signal transduction. Phosphoinositide properties are largely determined by the characteristics of their headgroup, which at physiological pH is highly charged but also capable of forming hydrogen bonds. Many proteins have developed special binding domains that facilitate specific binding to particular phosphoinositides, while other proteins interact with phosphoinositides via nonspecific electrostatic interactions. Despite its importance, only limited information is available about the ionization properties of phosphoinositides. We have investigated the pH-dependent ionization behavior of all three naturally occurring phosphatidylinositol bisphosphates as well as of phosphatidylinositol 3,4,5-trisphosphate in mixed phosphoinositide/phosphatidylcholine vesicles using magic angle spinning <sup>31</sup>P NMR spectroscopy. For phosphatidylinositol 3,5-bisphosphate, where the two phosphomonoester groups are separated by a hydroxyl group at the 4-position, the pH-dependent chemical shift variation can be fitted with a Henderson–Hasselbalch-type formalism, yielding pK<sub>a2</sub> values of 6.96 ± 0.04 and 6.58 ± 0.04 for the 3- and 5-phosphates, respectively. In contrast, phosphatidylinositol 3,4-bisphosphate [PI(3,4)P<sub>2</sub>] as well as phosphatidylinositol 4,5-bisphosphate [PI(4,5)P<sub>2</sub>] show a biphasic pH-dependent ionization behavior that cannot be explained by a Henderson–Hasselbalch-type formalism. This biphasic behavior can be attributed to the sharing of the last remaining proton between the vicinal phosphomonoester groups. At pH 7.0, the overall charge (including the phosphodiester group charge) is found to be −3.96 ± 0.10 for PI(3,4)P<sub>2</sub> and −3.99 ± 0.10 for PI(4,5)P<sub>2</sub>. While for PI(3,5)P<sub>2</sub> and PI(4,5)P<sub>2</sub> the charges of the individual phosphate groups in the molecule differ, they are equal for PI(3,4)P<sub>2</sub>. Differences in the charges of the phosphomonoester groups can be rationalized on the basis of the ability of the respective phosphomonoester group to form intramolecular hydrogen bonds with adjacent hydroxyl groups. Phosphatidylinositol 3,4,5-trisphosphate shows an extraordinary complex ionization behavior. While at pH 4 the <sup>31</sup>P NMR peak of the 4-phosphate is found downfield from the other two phosphomonoester group peaks, an increase in pH leads to a crossover of the 4-phosphate, which positions this peak eventually upfield from the other two peaks. As a result, the 4-phosphate group shows a significantly lower charge at pH values between 7 and 9.5 than the other two phosphomonoester groups. The charge of the respective phosphomonoester group in PI(3,4,5)P<sub>3</sub> is lower than the corresponding charge of the phosphatidylinositol bisphosphate phosphomonoester groups, leading to an overall charge of PI(3,4,5)P<sub>3</sub> of −5.05 ± 0.15 at pH 7.0. The charge of all investigated phosphoinositides at pH 7.0 is equal or higher than the corresponding charge of soluble inositol polyphosphate headgroup analogues, which is the opposite of what is expected on the basis of simple electrostatic considerations. This higher than expected headgroup charge can be rationalized with mutual intermolecular hydrogen bond formation. Measurements using different concentrations of PI(4,5)P<sub>2</sub> in the lipid vesicles (1, 5, and 20 mol %) did not reveal any significant concentration-dependent shift of the two phosphomonoester peaks, suggesting that PI(4,5)P<sub>2</sub> is clustered even at 1 mol %.

Phosphoinositides have been shown to mediate a large variety of important physiological processes by affecting the activity and/or localization of membrane-associated proteins. The high specificity of phosphoinositide–protein interactions (1, 2), the preferred accumulation of specific phosphoinositide derivatives in certain cellular compartments (3), and the laterally nonuniform distribution of phosphoinositides (4) are rooted in the rich chemical functionality of their headgroup, which exhibits for

each phosphoinositide derivative a distinct hydroxyl/phosphomonoester substitution pattern at the inositol ring (Figure 1).

Phosphatidylinositol 4,5-bisphosphate [PI(4,5)P<sub>2</sub>]<sup>1</sup> is by far the most abundant of all phosphoinositides [~1% of all membrane

<sup>†</sup>This work was supported by an award from the Ohio Board of Regents, National Science Foundation Grant CHEM 0724082, and a Farris Family Fellowship to E.E.K.

\*To whom correspondence should be addressed: Department of Chemistry, Kent State University, P.O. Box 5190, Kent, OH 44242. Phone: (330) 672-2986. Fax: (330) 672-3816. E-mail: agericke@kent.edu.

<sup>1</sup>Abbreviations: PI(3,5)P<sub>2</sub>, phosphatidylinositol 3,5-bisphosphate; PI(3,4)P<sub>2</sub>, phosphatidylinositol 3,4-bisphosphate; PI(4,5)P<sub>2</sub>, phosphatidylinositol 4,5-bisphosphate; PI(3,4,5)P<sub>3</sub>, phosphatidylinositol 3,4,5-trisphosphate; PC, phosphatidylcholine; DO, dioleoyl; PA, phosphatidic acid; LPA, lysophosphatidic acid; PE, phosphatidylethanolamine; PI, phosphatidylinositol; MAS, magic angle spinning; NMR, nuclear magnetic resonance; CSA, chemical shift anisotropy; CP, cross polarization; PTEN, phosphatase and tensin homologue deleted on chromosome 10; PIP5K, phosphatidylinositol 4-phosphate 5-kinase; PIP4K, phosphatidylinositol 5-phosphate 4-kinase; SHIP1 and -2, Src homology 2 domain containing inositol polyphosphate 5-phosphatases 1 and 2, respectively; PIKfyve, phosphatidylinositol 3-phosphate 5-kinase.

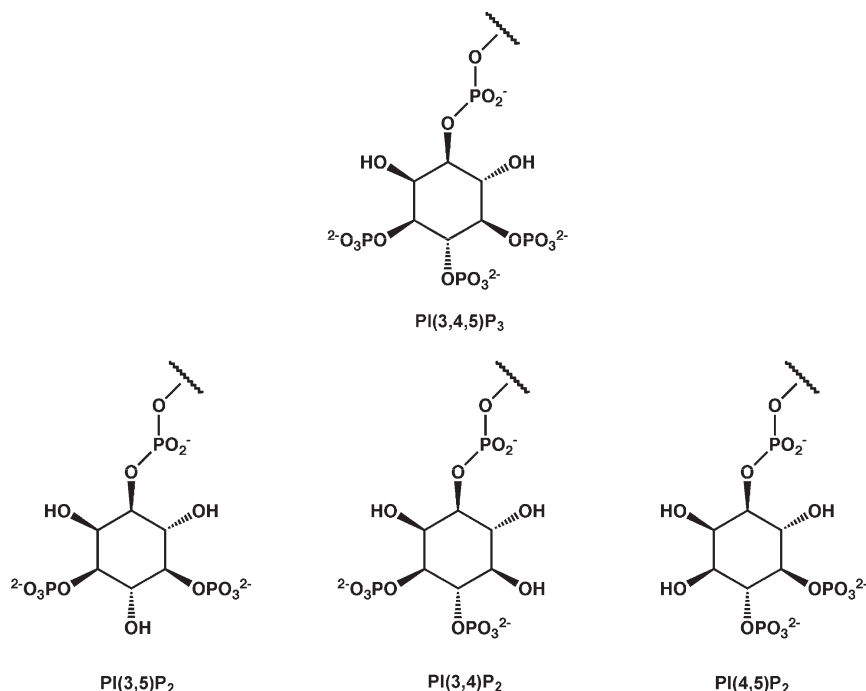


FIGURE 1: Headgroup structures of phosphatidylinositol polyphosphates. The fully ionized form of the lipid headgroup is shown. At physiological pH, the phosphomonoester groups are partially protonated. The 2-OH group is axial, while all other OH and phosphomonoester groups are equatorial. Inositol ring positions are counted counterclockwise from 1 to 6, starting at the phosphodiester.

phospholipids (5)] and is found primarily at the cytoplasmic leaflet of the plasma membrane. Two distinct pathways lead to the formation of PI(4,5)P<sub>2</sub>: first phosphorylation of PI(4)P by type I phosphatidylinositol 4-phosphate 5-kinases (PIP5Ks) and, second phosphorylation of PI(5)P by type II phosphatidylinositol 5-phosphate 4-kinases (PIP4Ks) (6). PI(4,5)P<sub>2</sub> levels are determined by a balance between synthesis and dissipation. The amount of PI(4,5)P<sub>2</sub> in the plasma membrane can be decreased in a variety of ways: The hydrolysis of PI(4,5)P<sub>2</sub> by phospholipase C leads to the formation of inositol 1,4,5-trisphosphate and diacylglycerol, which are both second-messenger molecules affecting Ca<sup>2+</sup> release and inflammatory response (7–9). In addition, the phosphomonoester group at the 5-position of the inositol ring can be dephosphorylated by phosphoinositide 5-phosphatases like synaptojanin and Ocr1 (10). PI(4,5)P<sub>2</sub> is involved in many physiological processes (11), including membrane trafficking events, cytoskeletal remodeling (12), and chemotaxis (4) as well as ion channel and transporter functions (13).

The phosphorylation of PI(4,5)P<sub>2</sub> by class I PI 3-kinases leads to the formation of phosphatidylinositol 3,4,5-trisphosphate [PI(3,4,5)P<sub>3</sub>], which is a second-messenger molecule that controls a broad range of membrane trafficking events (14). PI(3,4,5)P<sub>3</sub> has been shown to affect physiological processes like cell survival and cell proliferation (15), cytokinesis (4), and glucose transport (16). Dysregulation of cellular PI(3,4,5)P<sub>3</sub> levels has been associated with several disease states, most notably cancer (17, 18). Basal PI(3,4,5)P<sub>3</sub> levels are controlled by PTEN, which is an important tumor suppressor protein that converts PI(3,4,5)P<sub>3</sub> back to PI(4,5)P<sub>2</sub> (19).

Phosphatidylinositol 3,4-bisphosphate [PI(3,4)P<sub>2</sub>] is obtained through dephosphorylation of PI(3,4,5)P<sub>3</sub> by a variety of 5-phosphatases, most notably, SHIP1 and SHIP2 (Src homology 2 domain containing inositol polyphosphate 5 phosphatases 1 and 2, respectively) (20). In contrast to PTEN, which keeps the basal levels of PI(3,4,5)P<sub>3</sub> low, it is believed that the SHIP phosphatases

reduce acute PI(3,4,5)P<sub>3</sub> levels. PI(3,4)P<sub>2</sub> is also synthesized directly from PI(4)P by the non-receptor-regulated class II PI 3-kinases (21). The physiological functions of distinct PI(3,4)P<sub>2</sub> pools are only beginning to emerge; however, recent evidence suggests that PI(3,4)P<sub>2</sub> is an important independent lipid signal. First, it has been shown that PI(3,4)P<sub>2</sub> levels correlate with Akt phosphorylation at Ser473, while PI(3,4,5)P<sub>3</sub> levels impact phosphorylation at Thr308 (22). Second, type I and II inositol polyphosphate 4-phosphatases exhibit a strong *in vitro* preference for PI(3,4)P<sub>2</sub> over other phosphoinositides. Loss of type I inositol polyphosphate 4-phosphatase leads to enhanced PI(3,4)P<sub>2</sub> levels associated with a severe phenotype of neuronal loss in the cerebellum, ataxia, and neonatal death in a mutant mouse model (23, 24). Finally, several proteins bind with high specificity to PI(3,4)P<sub>2</sub> (25, 26), suggesting that this lipid has precise molecular targets with distinct physiological functions.

Phosphatidylinositol 3,5-bisphosphate [PI(3,5)P<sub>2</sub>] has been primarily associated with endosomal compartments (27). It has been proposed that PI(3,5)P<sub>2</sub> defines specific endosome platforms at the onset of the degradation pathway (28), and it has been suggested that PI(3,5)P<sub>2</sub> is important for endosome formation, morphology, and cargo flux (29). PI(3,5)P<sub>2</sub> is solely obtained through phosphorylation of PI(3)P by PIKfyve (29–31), while Sac3 dephosphorylates PI(3,5)P<sub>2</sub> back to PI(3)P (32). Myotubularins are phosphatases specific for the 3-position of the phosphoinositide headgroup that have been shown to dephosphorylate PI(3,5)P<sub>2</sub> to PI(5)P (33). Dysregulation of endosomal PI(3,5)P<sub>2</sub> levels has been associated with neurodegeneration in mice (34) and a variety of human diseases like corneal fleck dystrophy, Charcot-Marie-Tooth disease, and various forms of neuropathy (35).

Phosphoinositide properties are largely determined by the characteristics of their headgroup, which at physiological pH is highly charged but also capable of forming hydrogen bonds. The spatiotemporal control of phosphoinositide-mediated signaling

events requires the local enrichment of phosphoinositides, which will depend on the interplay between attractive and repulsive forces. The binding of phosphoinositides to proteins with distinct binding pockets (1, 2), the electrostatic interaction with positively charged proteins (5) or bivalent cations, and the mutual phosphoinositide interaction and the interaction with other lipid species are intimately linked to the ionization state of the respective phosphoinositide.

The ionization properties of PI(4)P and PI(4,5)P<sub>2</sub> in micelles and in PC/phosphoinositide vesicles have been previously investigated (36). It was found for PI(4,5)P<sub>2</sub> that the pK<sub>a2</sub> values differed for the phosphomonoester groups at the 4- and 5-positions of the inositol ring [6.5 and 7.7, respectively, mixed PC/PI(4,5)P<sub>2</sub> small unilamellar vesicles]. The same study also revealed that the pK<sub>a2</sub> value of the phosphomonoester group at the 4-position is lower for PI(4)P (6.1) than for PI(4,5)P<sub>2</sub> (6.5), suggesting that the chemical nature of the groups vicinal to the phosphomonoester group affect its ionization properties. In a series of papers starting in the early 1990s, Spiess and co-workers explored this aspect in great detail by investigating the pH-dependent ionization behavior of various types of inositol polyphosphates with <sup>1</sup>H and <sup>31</sup>P NMR spectroscopy (37). They found that neighboring phosphomonoester groups, as they are found in inositol 4,5-bisphosphate, will share the last remaining proton, which leads to a nonmonotonic behavior of the pH-dependent phosphorus chemical shift variation for the respective phosphomonoester group (38). In addition, vicinal hydroxyl groups form hydrogen bonds with the phosphomonoester groups, resulting in a reduced level of repulsion of the partially deprotonated phosphomonoesters (39–41). This hydrogen bond formation was found to be significantly stronger for *trans* diequatorial hydroxyl/phosphomonoester pairs than for *cis*-oriented axial/equatorial hydroxyl/phosphomonoester combinations.

The ionization properties of phosphoinositides in lipid bilayers are significantly more complex than those observed for inositol polyphosphates. The increased charge density at the bilayer–water interface leads to an altered ionization behavior of the inositol headgroup in comparison to the analogous inositol polyphosphate. Most importantly, phosphoinositides might form mutual hydrogen bonds or might interact with other hydrogen donors (e.g., PE) present in the membrane as found for phosphatidic acid (42). Ultimately, the ionization state of the phosphoinositide headgroup will be an important factor for phosphoinositide–protein interactions, regardless of whether these interactions are specific or nonspecific electrostatic. This study is driven by the hypothesis that the ionization behavior of phosphoinositides is strongly dependent on the molecular geometry of the headgroup, i.e., whether the respective phosphomonoester group is *cis* or *trans* to neighboring hydroxyl groups and whether the respective phosphomonoester group is isolated or adjacent to another phosphomonoester group. To explore these questions, we investigate by magic angle spinning (MAS) solid state <sup>31</sup>P NMR the pH-dependent ionization of the three naturally occurring phosphatidylinositol bisphosphates PI(3,5)P<sub>2</sub>, PI(3,4)P<sub>2</sub>, and PI(4,5)P<sub>2</sub> and of the only phosphatidylinositol trisphosphate found in biological membranes, PI(3,4,5)P<sub>3</sub>.

We also aim to address some discrepancies present in the current literature. Van Paridon et al. (36) did not observe the sharing of the last proton in PI(4,5)P<sub>2</sub> which was found by the Spiess group for the soluble analogue Ins(4,5)P<sub>2</sub> and other

inositol polyphosphates with vicinal phosphomonoester groups (37). However, because of experimental limitations at the time, van Paridon et al. were not able to inspect the pH range around the pK<sub>a2</sub> in sufficient detail to be able to judge whether the last remaining hydrogen was shared. By carefully resolving the pH range around the pK<sub>a2</sub> of the respective phosphoinositide, we are able to show that also phosphoinositides share the last remaining proton if the phosphomonoester groups are vicinal.

## MATERIALS AND METHODS

**Sample Preparation.** 1,2-Dioleoyl-*sn*-glycero-3-phosphatidylcholine (DOPC), 1,2-dioleoyl-*sn*-glycero-3-phosphatidylinositol 4,5-bisphosphate (triammonium salt) [DOPI(4,5)P<sub>2</sub>], L- $\alpha$ -phosphatidylinositol 4,5-bisphosphate (brain, porcine-triammonium salt) [brain PI(4,5)P<sub>2</sub>], 1,2-dioleoyl-*sn*-glycero-3-phosphatidylinositol 3,4-bisphosphate (triammonium salt) [DOPI(3,4)P<sub>2</sub>], 1,2-dioleoyl-*sn*-glycero-3-phosphatidylinositol 3,5-bisphosphate (triammonium salt) [DOPI(3,5)P<sub>2</sub>], and 1,2-dioleoyl-*sn*-glycero-3-phosphatidylinositol 3,4,5-trisphosphate (triammonium salt) [DOPI(3,4,5)P<sub>3</sub>] were purchased from Avanti Polar Lipids (Birmingham, AL). Phosphatidylinositol lipids were dissolved in chloroform, methanol, and water in a 20:9:1 volume ratio and were used as they were received from Avanti. The lipid purity of the DOPC stock for preparing the samples was regularly checked by HPTLC plates and judged to be better than 99%, one single spot on an iodine-stained plate. Water used in the experiments came from a Milli-Q system (Millipore, Bedford, MA), had a resistivity of 18.2 M $\Omega$  cm, or was of HPLC grade and purchased from Fisher Scientific.

NMR samples, for pH titration purposes, were prepared by mixing appropriate amounts of lipid stock. The two lipid components used for the preparation of the vesicles were matched with respect to their acyl chain composition. Briefly, 2 mg of DOPI(*x,y*)P<sub>2</sub> [PI(*x,y*)P<sub>2</sub>: PI(3,5)P<sub>2</sub>, PI(3,4)P<sub>2</sub>, or PI(4,5)P<sub>2</sub>] or DOPI(3,4,5)P<sub>3</sub> was dissolved in 1 mL of a 20:9:1 chloroform/methanol/water mixture, and 100  $\mu$ L aliquots [0.186  $\mu$ mol, 0.171  $\mu$ mol for PI(3,4,5)P<sub>3</sub>] were divided into 10 individual sample vials, mixed with 3.54  $\mu$ mol [3.25  $\mu$ mol for PI(3,4,5)P<sub>3</sub>] of DOPC from a chloroform/methanol mixture (2:1), subsequently dried under a stream of N<sub>2</sub> at 40–50 °C, and kept at 40–50 °C under high vacuum overnight. Lipid films consisting of 95 mol % PC and 5 mol % phosphoinositide (total of 3.72  $\mu$ mol) were hydrated at room temperature using 2.0 mL of the appropriate buffer to yield a final concentration of 1.86 mM. The following buffers were used: 20 mM citric acid, 30 mM MES (4 < pH < 6.7), 50 mM Tris (6.7 < pH < 8.5), and 50 mM CHES (8.5 < pH < 10). They contained 100 mM NaCl and 2 mM EDTA to complex any traces of divalent cations. The samples were vortexed for at least 1 min to ensure full dispersion of the lipid film in the buffer. The pH of the lipid dispersion was measured with a Sentron intelli probe (RL Instruments, Manchaug, MA) on a standard pH meter, which is particularly well-suited for samples with high lipid concentrations. This pH, measured after lipid hydration, was used to construct the pH titration curves. The lipid dispersions were concentrated in a tabletop centrifuge (14900 rpm for 1 h at room temperature), and the (wet) lipid pellet was transferred to 4 mm zirconium MAS NMR sample tubes.

Alternatively, lipid films consisting of 0.227  $\mu$ mol of brain PI(4,5)P<sub>2</sub> and 4.31  $\mu$ mol of DOPC were prepared in a rotary evaporator using specially made borosilicate glass tubes (15 mm test tube size). Specifically, 50  $\mu$ L of a 4.554  $\mu$ mol/mL phosphoinositide



(5 mg in 1 mL of solvent) stock solution was mixed with 317  $\mu$ L of 13.6  $\mu$ mol/mL DOPC in a 2:1 chloroform/methanol mixture and  $\sim$ 600  $\mu$ L of HPLC grade chloroform using a vortexer. This mixture was dried to a thin lipid film on the bottom of the borosilicate test tube in the rotary evaporator setup at 45  $^{\circ}$ C. Lipid stocks and films were kept under an inert atmosphere of  $N_2$  gas during sample preparation. Hydrated lipid samples were prepared as detailed above. This sample preparation (preparation of the lipid film in a test tube using the rotary evaporator and extra addition of chloroform) proved to be sufficient to remove the splitting observed in the phosphomonoester peaks of PI(4,5)P<sub>2</sub> and PI(3,4,5)P<sub>3</sub> when the sample was prepared using the procedure described in the previous paragraph. The additional peaks most likely originate from a metastable state formed by PI(4,5)P<sub>2</sub> and PI(3,4,5)P<sub>3</sub> using that sample preparation method. Details of this experimental finding are further discussed in the Supporting Information. Aside from the improved sample preparation method using the rotary evaporator discussed above, the splitting of PI(4,5)P<sub>2</sub> and PI(3,4,5)P<sub>3</sub> phosphomonoester peaks could also be removed by a simple freeze–thaw procedure. Briefly, hydrated lipid suspensions were flash-frozen in dry ice-cooled ethanol and subsequently warmed to room temperature, while the suspension was occasionally vortexed while it thawed. This procedure homogenizes the lipid suspension and removes any metastable states formed during lipid film preparation and subsequent hydration.

**NMR Spectroscopy.**  $^{31}$ P NMR spectra were recorded on a Bruker (Karlsruhe, Germany) DMX 400 MHz widebore spectrometer at 161.97 MHz, using a 4 mm cross-polarization (CP) MAS NMR probe. Experiments were conducted using two different observer pulse widths (3.5 and 7.5  $\mu$ s) as well as two different decoupling conditions (static experiments only,  $^1$ H 90 $^{\circ}$ , 30 and 60  $\mu$ s) and deployed a delay time of 1 s between pulses. Samples were spun at the magic angle (54.7 $^{\circ}$ ) at 5 kHz to average the chemical shift anisotropy, and the chemical shift position of the lipids was recorded relative to an external 85%  $H_3PO_4$  standard. Under stable spinning conditions, typically, 60000–100000 scans were recorded for the oleoyl-containing PI(x,y)P<sub>2</sub> and PI(3,4,5)P<sub>3</sub> samples and between 20000 and 60000 scans were recorded for the brain PI(4,5)P<sub>2</sub>-containing samples [the brain PI(4,5)P<sub>2</sub> samples contained more lipid, hence the shorter experimental time]. Experiments were conducted at 25.0  $\pm$  1.0  $^{\circ}$ C. Static spectra, using low-power proton decoupling (using the WALTZ16 pulse program), were recorded in the same 4 mm CP MAS NMR probe, after the MAS spectra had been recorded. Typically, between 70000 and 200000 scans were recorded.

**Determination of  $pK_a$  Values and Phosphoinositide Headgroup Charges.** The  $pK_{a2}$  values for the phosphomonoester groups of PI(3,5)P<sub>2</sub> were determined using eq 1, which was derived from the Henderson–Hasselbalch equation using the assumption that the observed chemical shift values are weighted averages of the chemical shifts of the singly dissociated and doubly dissociated states (43). The  $pK_{a2}$  values are determined utilizing a nonlinear least-squares fit procedure.

$$\delta = \frac{\delta_A \times 10^{pK_{a2} - pH} + \delta_B}{1 + 10^{pK_{a2} - pH}} \quad (1)$$

where  $\delta_A$  and  $\delta_B$  are the chemical shifts of the singly dissociated and doubly dissociated states, respectively,  $\delta$  is the measured pH-dependent chemical shift, and  $pK_{a2}$  is the second dissociation constant of the respective phosphomonoester. This approach,

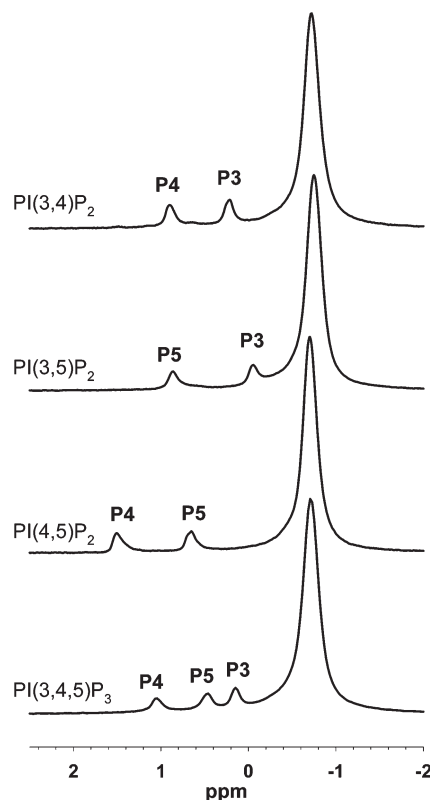


FIGURE 2: Peak assignment for PI(3,4,5)P<sub>3</sub>, PI(3,4)P<sub>2</sub>, and PI(3,5)P<sub>2</sub>. Raw  $^{31}$ P MAS NMR spectra for (from top to bottom) 5 mol % dioleoyl-PI(3,4)P<sub>2</sub>, dioleoyl-PI(3,5)P<sub>2</sub>, dioleoyl-PI(4,5)P<sub>2</sub>, and dioleoyl-PI(3,4,5)P<sub>3</sub> in DOPC at pH 4.3. The phosphomonoester peaks for PI(4,5)P<sub>2</sub> were assigned previously (36).

where only the upper part of the titration curve (second dissociation step) is measured and analyzed, does not significantly affect the  $pK_{a2}$  value as demonstrated previously (42).

Equation 1 was not suitable for fitting the data for PI(4,5)P<sub>2</sub>, PI(3,4)P<sub>2</sub>, or PI(3,4,5)P<sub>3</sub>. In these cases, we calculated the degree of protonation  $f$  as a function of pH by using eq 3. Like for eq 1, eqs 2 and 3 are rooted in the assumption that the chemical shift values are the weighted averages between the singly and completely deprotonated states of the respective phosphomonoester groups.

$$\delta_i^{\text{obs}} = f_{i,p} \delta_{i,p} + (1 - f_{i,p}) \delta_{i,d} \quad (2)$$

where  $\delta_i^{\text{obs}}$  is the pH-dependent chemical shift of phosphomonoester group  $i$  and  $\delta_{i,p}$  and  $\delta_{i,d}$  are the chemical shifts of the singly protonated and completely deprotonated phosphomonoester groups, respectively (37). Equation 2 can be rearranged to

$$f_{i,p} = \frac{\delta_i^{\text{obs}} - \delta_{i,d}}{\delta_{i,p} - \delta_{i,d}} \quad (3)$$

## RESULTS

Phosphorus ( $^{31}$ P) NMR has been used extensively to determine ionization constants for phosphate groups in glycerophospholipids and sphingolipids (36, 42, 44–47). Most of these studies relied on the use of small vesicles or micelle solutions since these give rise to high-resolution  $^{31}$ P NMR spectra (36, 44–46). Phospholipids dispersed in extended, multilamellar vesicles display a large chemical shift anisotropy that masks pH-dependent ionization changes. This problem can be overcome by the use of

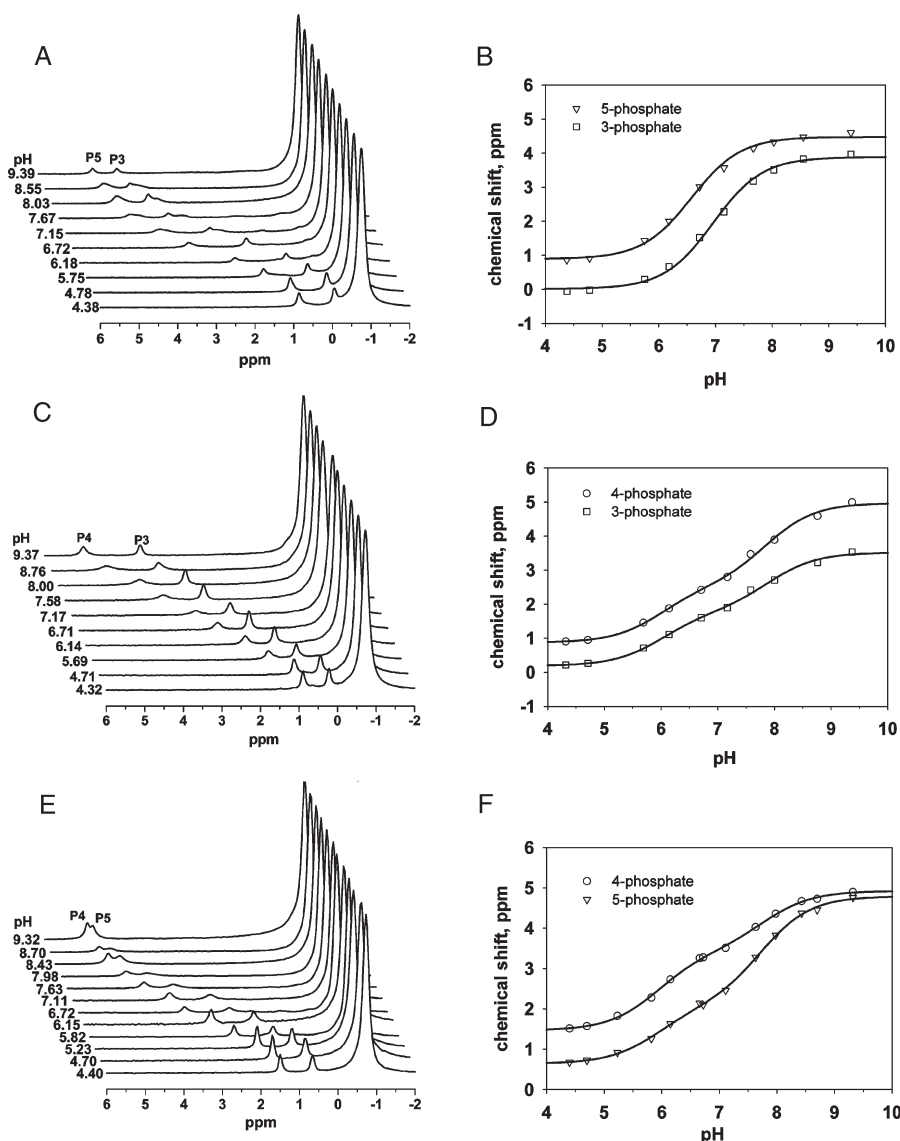


FIGURE 3:  $^{31}\text{P}$  MAS NMR spectra and pH titration curves for  $\text{PI}(x,y)\text{P}_2$  in DOPC vesicles. (A)  $^{31}\text{P}$  MAS NMR spectra as a function of pH for 5 mol % dioleoyl- $\text{PI}(3,5)\text{P}_2$  in DOPC. (B) Peak positions of the 3- and 5-phosphates of  $\text{PI}(3,5)\text{P}_2$  plotted as a function of pH. Solid lines represent nonlinear least-squares fits of the data to eq 1 (see Materials and Methods). (C)  $^{31}\text{P}$  MAS NMR spectra as a function of pH for 5 mol % dioleoyl- $\text{PI}(3,4)\text{P}_2$  in DOPC. (D) Peak positions of the 3- and 4-phosphates of  $\text{PI}(3,4)\text{P}_2$  plotted as a function of pH. (E)  $^{31}\text{P}$  MAS NMR spectra as a function of pH for 5 mol % brain  $\text{PI}(4,5)\text{P}_2$  in DOPC. (F) Peak positions of the 4- and 5-phosphates of  $\text{PI}(4,5)\text{P}_2$  plotted as a function of pH. Solid lines in D and F are meant to guide the eye to accentuate the biphasic ionization behavior of these  $\text{PI}(x,y)\text{P}_2$  lipids.

magic angle spinning (MAS)  $^{31}\text{P}$  NMR. MAS NMR allows for the acquisition of high-resolution chemical shift data of physiologically relevant extended and multilamellar and multicomponent vesicles (48, 49). Previous work has clearly shown the feasibility of this approach for the characterization of acidic lipids in mixtures with other lipids (42, 47, 50).

To be able to study phosphoinositides at low concentrations in vesicles, they were mixed with a bilayer-forming lipid, DOPC, which was chosen as the "matrix" lipid since it gives rise to fluid (liquid crystalline) membranes, is zwitterionic (noncharged), and is not able to form hydrogen bonds with the respective phosphoinositide. Finally, the use of DOPC allows for the direct comparison with previous data (phosphatidic acid (PA), lysophosphatidic acid (LPA), dehydroxy-LPA, and ceramide 1-phosphate (Cer-1-P)) (42, 47, 50). Figure 2 shows the  $^{31}\text{P}$  MAS NMR spectra of 5 mol %  $\text{PI}(3,5)\text{P}_2$ ,  $\text{PI}(3,4)\text{P}_2$ ,  $\text{PI}(4,5)\text{P}_2$ , and  $\text{PI}(3,4,5)\text{P}_3$  in DOPC vesicles at a relatively low pH ( $\sim 4.3$ ). These data clearly demonstrate the high resolution that can be attained for phos-

phoinositides in multilamellar vesicles of DOPC, as the individual peaks for the respective phosphomonoester groups of the inositol ring are clearly resolved. The phosphodiester peak of the respective phosphoinositide essentially overlaps with the major high-field peak associated with the phosphodiester group of DOPC. Occasionally, a small shoulder on the low-field side of the DOPC peak can be observed, which can be assigned to the phosphodiester group of the phosphoinositide [e.g., see Figure 3C (pH 9.37)]. The assignment of the phosphomonoester peaks for the respective phosphoinositide was based upon previously established assignments for  $\text{PI}(4,5)\text{P}_2$  (36) as well as assignments derived for inositol polyphosphates (37). According to these assignments, the 4-phosphate of  $\text{PI}(4,5)\text{P}_2$  falls downfield of the 5-phosphate. These peaks most closely match those of the two most downfield peaks of  $\text{PI}(3,4,5)\text{P}_3$ , which we therefore assign to the 4- and 5-phosphates as indicated in Figure 2. The 3-phosphate of  $\text{PI}(3,4,5)\text{P}_3$  appears to be most shielded and coincides largely with the high-field peak for  $\text{PI}(3,4)\text{P}_2$  and

PI(3,5)P<sub>2</sub>. The high-field position of the 3-phosphate peak indicates an increased level of protonation of this phosphomonoester group in comparison to the 4- and 5-phosphates, which will be discussed in more detail below. The assignments given above are in agreement with those previously obtained for a variety of inositol polyphosphates (37, 38, 40, 51, 52).

**Titration Curves for Phosphatidylinositol Bis- and Trisphosphates in Fluid PC Membranes.** First, we set out to determine the  $pK_{a2}$  values of dioleoyl-PI(3,5)P<sub>2</sub> [DOPI(3,5)P<sub>2</sub>] at a low (5 mol %) concentration in a DOPC matrix.  $pK_{a2}$  describes the second ionization constant of the two phosphomonoester groups of the PI(3,5)P<sub>2</sub> headgroup [from one to two negative charges per phosphomonoester (see Figure 1 for chemical structures)]. We investigated the pH-dependent chemical shift variation of DOPI(3,5)P<sub>2</sub> by preparing individual DOPC/DOPI(3,5)P<sub>2</sub> vesicle dispersions while varying the pH of the hydration buffer. Typically, 10 pH values dispersed between pH 4 and 9.5 were used, the pH interval in which the  $pK_{a2}$  is expected to fall (42, 47). Raw <sup>31</sup>P MAS NMR spectra as a function of pH for 5 mol % DOPI(3,5)P<sub>2</sub> in DOPC are shown in Figure 3A. We observe a clear pH-dependent downfield shift of both the 3- and 5-phosphate peaks with an increase in pH, which is expected for an increased level of deprotonation (ionization) of the respective phosphate group. As anticipated, the position of the DOPC phosphodiester peak is not affected in this pH range. Next, we plotted the chemical shifts of the respective phosphomonoester group as a function of pH (Figure 3B). Solid lines represent nonlinear least-squares fits to a Henderson–Hasselbalch-type equation [ $R^2 > 0.99$  (see eq 1 in Materials and Methods)]. The  $pK_{a2}$  value for the phosphomonoester group in the 3-position is found to be  $6.96 \pm 0.04$ , while the respective value for the 5-position was  $6.58 \pm 0.04$ ; the reported errors follow from the fitting procedure.

Next we determined the pH titration behavior for DOPC vesicles containing either 5 mol % PI(3,4)P<sub>2</sub> [DOPI(3,4)P<sub>2</sub>] or PI(4,5)P<sub>2</sub> [brain PI(4,5)P<sub>2</sub>]. The analysis of the pH-dependent chemical shift for DOPI(4,5)P<sub>2</sub> and brain PI(4,5)P<sub>2</sub> (mainly stearoyl/arachidonoyl acyl chains) did not reveal any significant differences in the ionization behavior of the two phosphate groups (see Figure S1 of the Supporting Information). Since stearoyl/arachidonoyl is the physiological chain composition, we give here the data for brain PI(4,5)P<sub>2</sub> [PI(3,5)P<sub>2</sub> and PI(3,4)P<sub>2</sub> were commercially not available with a stearoyl/arachidonoyl chain composition at the time this study was conducted]. Panels C and E of Figure 3 show the respective raw spectra as a function of pH, while panels D and F of Figure 3 show the chemical shift variations of the phosphomonoester groups as a function of pH. Although the phosphate peaks are well-resolved in both cases, the resulting ionization behavior of the phosphate groups cannot be described by eq 1 (Materials and Methods), and instead, a biphasic behavior of the pH-dependent chemical shift variation is observed. This biphasic behavior is most clear from the solid lines in the figure, which are only meant to guide the eye. Spiess and co-workers have shown in their studies of inositol polyphosphates that vicinal phosphate groups share the last remaining proton, resulting in a reduced level of ionization of the respective phosphate group, and a biphasic ionization is also observed (37, 41). This aspect will be further discussed below.

To determine whether the samples formed bilayers, we recorded static spectra for selected samples along the pH titration curve. A low-field shoulder and high-field peak are characteristic

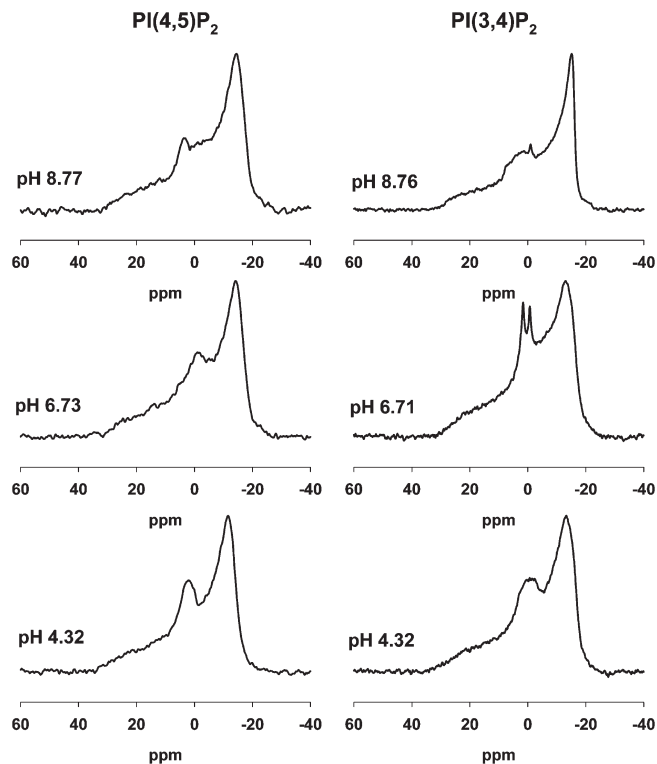


FIGURE 4: Static NMR spectra for selected pH values for PI(4,5)P<sub>2</sub> and PI(3,4)P<sub>2</sub>.

for static <sup>31</sup>P NMR spectra of lipid mixtures organized in a fluid bilayer (53). Figure 4 shows three spectra at different pH values for mixtures of 5 mol % PI(4,5)P<sub>2</sub> in DOPC, which confirm an organization of the lipids in a fluid lipid bilayer over the complete investigated pH range. Superimposed on these bilayer spectra is a broad isotropic-like “peak”, which most likely originates from smaller vesicles. This is inherent to lipid mixtures containing anionic lipids. The chemical shift anisotropy of the PI(4,5)P<sub>2</sub> phosphodiester is not resolved in these low-power proton-decoupled spectra but does show up for lipid mixtures containing more PI(4,5)P<sub>2</sub> (data not shown). Static experiments employing a larger amount of PI(4,5)P<sub>2</sub> thus confirm that the PI(4,5)P<sub>2</sub> is largely taken up in the DOPC bilayer. The chemical shift anisotropy of the PI(4,5)P<sub>2</sub> diester is ~69 ppm, i.e., considerably larger than the chemical shift anisotropy for DOPC, which is ~42 ppm as determined from our experiments (and consistent with the literature, e.g., ref 54).

Figure 4 shows static spectra for PI(3,4)P<sub>2</sub> for three pH values taken along the titration curve. These spectra also confirm the formation of fluid bilayers across the entire pH range investigated. More pronounced isotropic features do appear in some of these spectra, most notably for pH 6.71. The origin of these isotropic features is examined more fully in the Supporting Information.

The global concentration of PI(4,5)P<sub>2</sub> in biological membranes is ~1 mol % (5); however, the local concentration might exceed this value because of the formation of PI(4,5)P<sub>2</sub>-enriched membrane regions. Since the charge density affects the ionization properties of phosphomonoester groups, we investigated PI(4,5)P<sub>2</sub> ionization for different concentrations in the DOPC bilayer. We found for 1, 5, and 20 mol % that the chemical shift of the respective phosphomonoester group is largely unaffected by increasing PI(4,5)P<sub>2</sub> concentrations (see Figure SP2 of the Supporting Information). For phosphatidic acid (PA), it has

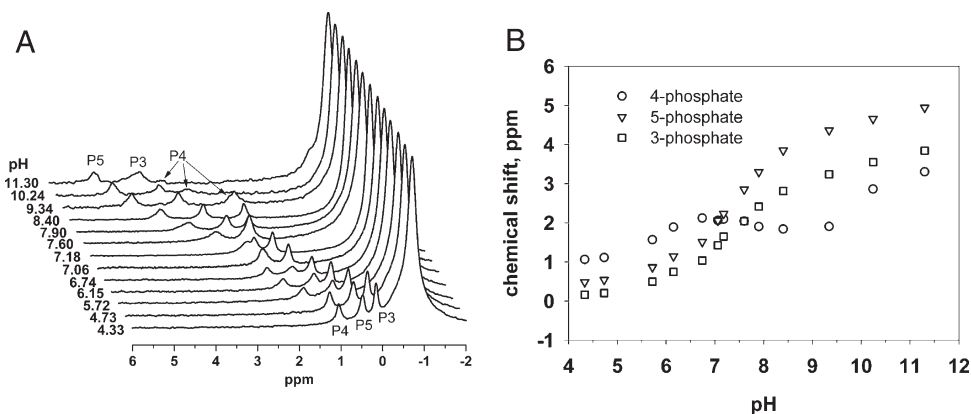


FIGURE 5:  $^{31}\text{P}$  MAS NMR spectra and derived pH titration curves for PI(3,4,5) $\text{P}_3$ . Assignments of the individual peaks are as discussed in the text.

previously been found that the ionization of the headgroup significantly decreases with increasing PA concentrations because of the increasing charge density; i.e., the phosphate peak shifted to the high field with an increase in PA concentration (46). The fact that the chemical shift values of the PI(4,5) $\text{P}_2$  4- and 5-phosphates are largely unaffected by increasing PI(4,5) $\text{P}_2$  concentrations suggests that the local environment of PI(4,5) $\text{P}_2$  is not changing, which might be indicative of a clustering of PI(4,5) $\text{P}_2$  (see below for further discussion).

Throughout our studies, we found that commonly employed vesicle sample preparation procedures [drying of lipids from organic solutions and resuspension in buffer solution (see Materials and Methods for details)] lead to the formation of metastable states that were associated with additional high-field peaks in the  $^{31}\text{P}$  NMR spectrum (see Figure SP1 of the Supporting Information); i.e., the phosphate groups were characterized by a reduced charge. We also found that the extent of formation of these metastable states was dependent on the nature of the phosphoinositide headgroup; e.g., PI(4,5) $\text{P}_2$  exhibited a strong tendency toward the formation of these states, while PI(3,4) $\text{P}_2$  showed no formation of these states as discerned by MAS  $^{31}\text{P}$  NMR. At this point, we can only speculate about the nature of these metastable states, but most importantly, the formation of these metastable states could be easily avoided by slight adjustments in the sample preparation procedure. We found that freeze–thaw cycles removed these states. Alternatively, we also found that preparing the samples by rotary evaporation of the solvent with the addition of more chloroform removed these additional peaks (for details, see Materials and Methods and the Supporting Information). It is worth mentioning that the presence of cholesterol prevented the formation of metastable states regardless of the sample preparation procedure (not shown).

Finally, we investigated the pH-dependent ionization behavior of DOPC vesicles containing 5 mol % PI(3,4,5) $\text{P}_3$ . Figure 5A shows the raw spectra as a function of pH. The NMR spectra reveal an extraordinary complex ionization behavior. At low pH, three peaks associated with the three phosphomonoester groups are readily discernible. With an increase in pH, the peaks become less separated and even partly superimpose between pH 7 and 8. This behavior has been observed before for Ins(1,3,4,5) $\text{P}_4$  (51, 55) and has been attributed to the fact that the 4-phosphate peak shifts upfield with respect to the two other phosphate peaks as the pH is being increased. This can be best seen in Figure 5B, which shows the chemical shifts of the respective phosphomonoester group as a function of pH. The unique ionization behavior of the 4-phosphate is a result of the fact that it is

neighbored by two phosphate groups, which is an aspect discussed further below.

## DISCUSSION

The data presented above clearly show that the protonation/deprotonation behavior of phosphoinositides is significantly more complex than previously thought and critically depends on the phosphate substitution pattern at the inositol ring. While the intramolecular hydrogen bond formation mirrors to some extent the hydrogen bonding pattern found for comparable inositol phosphate molecules, we also found some significant differences that can be attributed to the increased interfacial charge density of lipid bilayers as well as the formation of intermolecular hydrogen bonds. We will first discuss intramolecular hydrogen bond formation and then we will explore the question whether intermolecular interactions contribute to the observed ionization behavior of phosphoinositides.

The destabilizing effect of intramolecular hydrogen bond formation on the binding of the last remaining proton on a phosphomonoester headgroup has been previously established for phosphatidic acid (PA) and lysophosphatidic acid (LPA) (42). Compared to PA, LPA has a lower  $\text{p}K_{\text{a}2}$  value despite an identical phosphomonoester headgroup. The lower  $\text{p}K_{\text{a}2}$ , i.e., the higher degree of ionization at constant pH, is attributed to the free hydroxyl group in the backbone of LPA that forms an intramolecular hydrogen bond with the phosphomonoester headgroup. Indeed, deoxy-LPA that is lacking this hydroxyl group exhibited pH titration behavior identical to that of PA. These findings culminated in the electrostatic–hydrogen bond switch model describing the ionization properties of a phosphomonoester group (50). It is expected that the phosphomonoester groups in PI( $x,y$ ) $\text{P}_2$  and PI(3,4,5) $\text{P}_3$  behave in an identical manner.

**Phosphatidylinositol 3,5-Bisphosphate.** PI(3,5) $\text{P}_2$  has two isolated phosphate groups that cannot form mutual intramolecular hydrogen bonds (see Figure 6); i.e., the ionization behavior of a given phosphate group is less affected by the other phosphate than is found for the other investigated phosphoinositides. As a result, the pH-dependent chemical shift variation of both phosphomonoester groups can be fitted with a Henderson–Hasselbalch-type formalism. The  $\text{p}K_{\text{a}2}$  value for the phosphomonoester group in the 3-position is found to be  $6.96 \pm 0.04$ , while the respective value for the 5-position was  $6.58 \pm 0.04$ .

For PI(3,5) $\text{P}_2$ , an axial hydroxyl group in the 2-position and an equatorial hydroxyl group in the 4-position neighbor the phosphomonoester group in the 3-position, while the



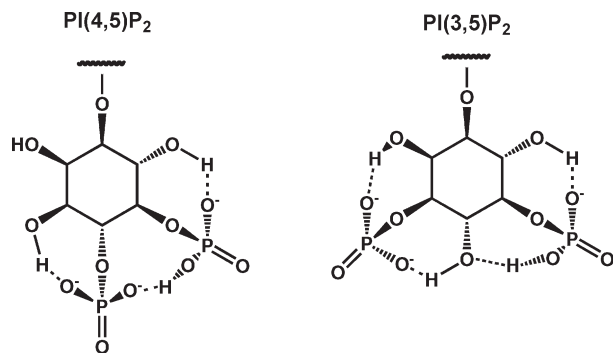


FIGURE 6: Schematic of intramolecular hydrogen bond formation in PI(3,5)P<sub>2</sub> and PI(4,5)P<sub>2</sub>.

phosphomonoester group in the 5-position is adjacent to two equatorial hydroxyl groups. It was previously found for inositol phosphates that a hydrogen bond formation for a *trans* diequatorial hydroxyl/phosphate group pair is significantly stronger than for a *cis* hydroxyl/phosphate axial/equatorial pair (39, 41). A suppressed ability to form hydrogen bonds between the respective phosphate group and the neighboring hydroxyl groups results in less stabilization of the completely deprotonated state of the phosphate group and hence a more tightly bound proton. Since the 3-phosphate group is *cis* to the 2-hydroxyl and *trans* to the 4-hydroxyl group, the proton of the phosphate group in the 3-position is more tightly bound than the proton associated with the phosphate group in the 5-position, which has a *trans/trans* orientation to both neighboring hydroxyl groups.

The difference in hydroxyl group position and subsequently the strength of the hydrogen bond formed yield at pH 7.0 a charge of approximately  $-1.52 \pm 0.05$  for the 3-position and  $-1.73 \pm 0.05$  for the 5-position as calculated from the  $pK_{a2}$  values, and an overall charge of  $-4.25 \pm 0.10$  (see Table 1 and also Figure 7A for the pH-dependent degree of protonation which results in identical charges as calculated from the  $pK_{a2}$  values), which is higher than what is found for the other two phosphatidylinositol bisphosphate derivatives (see Table 1). The reduced extent of hydrogen bond formation between the 3-phosphate and the hydroxyl group in the 2-position is also the reason for the upfield position of the 3-phosphate peak in comparison to the 5-phosphate peak.

Since no literature data are available for inositol 3,5-bisphosphate, the ionization behavior of PI(3,5)P<sub>2</sub> can be best compared to that of inositol 1,3,5-trisphosphate (37). Also in the case of Ins(1,3,5)P<sub>3</sub>, the phosphate groups exhibit an ionization behavior that can be described well with a Henderson–Hasselbalch-type formalism, the data for the 3-phosphate are found at lower ppm values than the corresponding 5-phosphate values, and the ppm difference between the singly protonated and completely deprotonated phosphate group is comparable to what is observed for PI(3,5)P<sub>2</sub>. The  $pK_{a2}$  values, however, are shifted to higher values in comparison to those of PI(3,5)P<sub>2</sub>, which will be discussed below in the context of intermolecular interactions.

**Phosphatidylinositol 4,5-Bisphosphate.** The pH-dependent chemical shift variation of PI(4,5)P<sub>2</sub> is characterized by two clearly discernible steps, which is an ionization behavior also found for inositol 4,5-bisphosphate [Ins(4,5)P<sub>2</sub>] (38). This bimodal behavior can be attributed to the sharing of the last remaining proton between the two vicinal phosphomonoester groups. The charges observed at pH 7.0 for PI(4,5)P<sub>2</sub> are  $-1.58 \pm 0.05$  (P4) and  $-1.41 \pm 0.05$  (P5) (see Figure 7B for the degree of protonation as a function of pH). The lower charge of the

phosphate group in the 5-position is most likely attributable to the fact that the hydroxyl group in the 6-position, which interacts with the phosphate group in the 5-position via hydrogen bonding, is also able to form a hydrogen bond with the phosphodiester group in the 1-position. As a result, the hydrogen bond between the hydroxyl group in the 6-position and the phosphate group in the 5-position is weakened and the proton on this phosphate group binds more tightly, leading to a charge lower than what is observed for the phosphate group at the 4-position. The weakened interaction of the phosphate group in the 5-position with the neighboring hydroxyl group is also reflected in the upfield position of the peak for the 5-phosphate in comparison to the corresponding peak for the 4-phosphate. The comparison of the charges observed for PI(4,5)P<sub>2</sub> at pH 7.0 ( $-1.58$  and  $-1.41$ , respectively) and those found for Ins(4,5)P<sub>2</sub> [ $-1.47$  and  $-1.34$ , respectively, derived from data presented by Schmitt et al. (38)] reveals also in this case a higher charge for the lipid than for the soluble inositol derivative, which will be discussed further below.

**Phosphatidylinositol 3,4-Bisphosphate.** Similar to the ionization behavior observed for PI(4,5)P<sub>2</sub>, the pH-dependent chemical shift variation of PI(3,4)P<sub>2</sub> is characterized by a bimodal behavior. Like for PI(4,5)P<sub>2</sub>, this biphasic behavior is associated with the sharing of the last proton between the two phosphomonoester groups. The charges for both phosphomonoester groups at pH 7.0 are found to be  $-1.48 \pm 0.05$  (see Figure 7C and Table 1). As found for PI(3,5)P<sub>2</sub>, the 3-phosphate peak is found upfield from the 4-phosphate peak, indicating less interaction with the hydroxyl group at the 2-position. However, while this leads in the case of PI(3,5)P<sub>2</sub> to a more strongly bound proton for the 3-phosphate, this is not the case for PI(3,4)P<sub>2</sub>. Apparently, the sharing of the last proton leads for PI(3,4)P<sub>2</sub> to a situation that is characterized by the same charge for the two phosphates for most of the pH range investigated, suggesting that the phosphate–phosphate interaction of two equatorial phosphomonoesters is stronger than the equatorial phosphate–axial hydroxyl group interaction.

**Phosphatidylinositol 3,4,5-Trisphosphate.** The pH-dependent chemical shift variation found for PI(3,4,5)P<sub>3</sub> reveals an extraordinary complex ionization behavior [see Figure 7D for the pH-dependent degree of protonation and Figure 7E for the total charge of PI(3,4,5)P<sub>3</sub> as a function of pH], which is similar to the ionization properties previously found for the soluble analogue Ins(1,3,4,5)P<sub>4</sub> (51, 55, 56). The complexity of the ionization behavior can be attributed to the fact that the central 4-phosphate can form hydrogen bonds with the vicinal 3- and 5-phosphates; however, it is not neighbored by any hydroxyl group. With an increase in the pH from 4 to  $\sim 6.5$ , the three peaks associated with the 3-, 4-, and 5-phosphate groups shift downfield, indicating for all three phosphate groups a decreasing degree of protonation (increased charge). At pH  $\sim 7$ – $7.5$ , the degree of protonation for the 4-phosphate reaches a local minimum, and with a further increase in pH, the degree of protonation increases until a pH of  $\sim 9.5$  is reached. In other words, the charge of the 4-phosphate is lower at pH 8 than at pH 7. In contrast, the degree of protonation for the 3- and 5-phosphates does not reach a minimum around pH 7 and increases instead more or less monotonically with pH. As a result, the 4-phosphate peak, which is initially downfield from the other two phosphomonoester peaks, crosses the other two peaks and eventually is found upfield from the 3- and 5-phosphate peak. The ionization behavior found for the 4-phosphate is typical for the central phosphate of inositol phosphates with three vicinal, equatorial phosphates. Similar



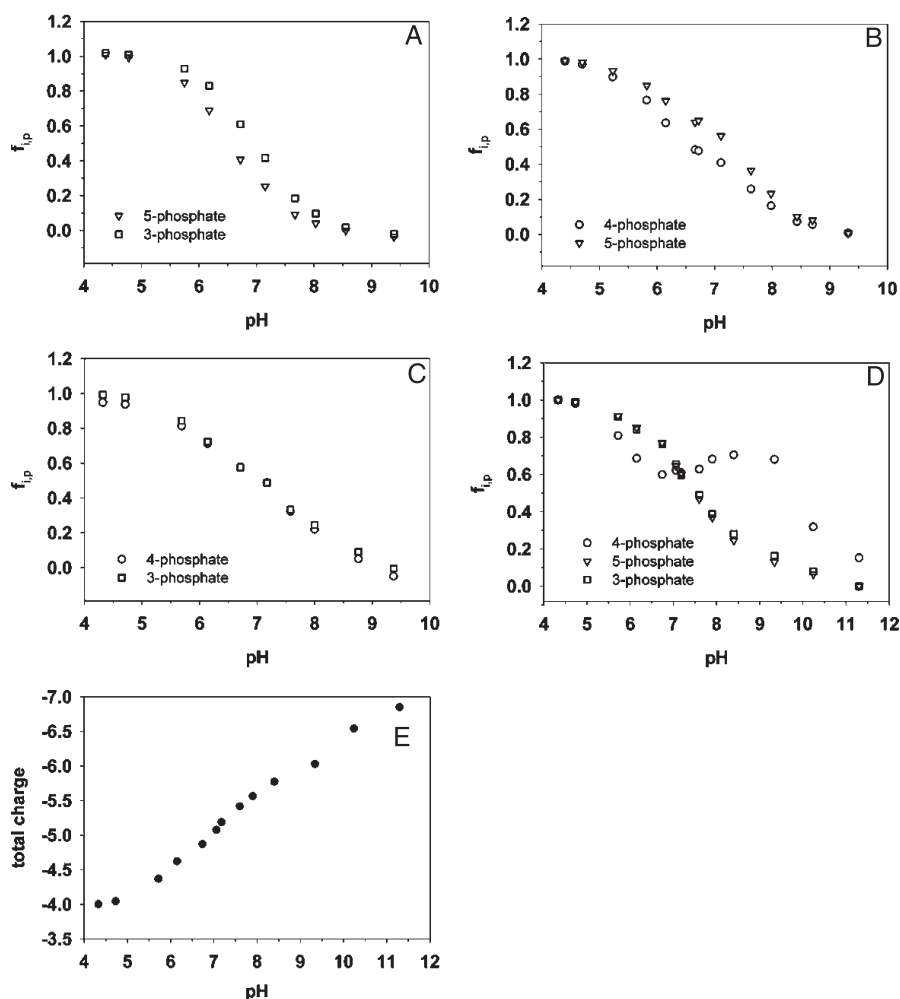


FIGURE 7: Degree of protonation as a function of pH for phosphoinositides (5%) in DOPC: (A) DOPI(3,5)P<sub>2</sub>, (B) brain PI(4,5)P<sub>2</sub>, (C) DOPI(3,4)P<sub>2</sub>, and (D) DOPI(3,4,5)P<sub>3</sub>. Subsequently, panel E shows the total charge of PI(3,4,5)P<sub>3</sub> as a function of pH. The degrees of protonation are calculated from the data in Figure 3 using eq 2. Chemical shift values at pH ~4.3 were taken as the singly dissociated values and those at pH ~10 as fully dissociated, except for DOPI(3,4,5)P<sub>3</sub> where the degree of ionization had to be determined at higher pH values. The chemical shift of the fully dissociated 4-phosphate is estimated to be ~3.7 ppm, as it is not possible to determine experimentally because of the apparent very high  $pK_a$  for the last remaining proton of this phosphomonoester.

ionization properties were found for Ins(1,3,4,5)P<sub>4</sub> (51, 55, 56) as well as Ins(4,5,6)P<sub>3</sub> (57). In contrast to those of the 3- and 5-phosphates, the charge on the 4-phosphate is not stabilized through hydrogen bond formation with adjacent hydroxyl groups, and therefore, the 4-phosphate will bind the last remaining proton most tightly, which is the reason for the increase in the degree of protonation between pH ~7 and ~9.5. It is striking that the charge of the individual phosphate groups in PI(3,4,5)P<sub>3</sub> is smaller than the charges found for the corresponding phosphate groups in phosphatidylinositol bisphosphates (see Table 1), resulting in a lower than expected overall charge ( $-5.05 \pm 0.15$ ) for the lipid. The degree of protonation  $f$  and the resulting charges observed for PI(3,4,5)P<sub>3</sub> at pH 7.0 (P3,  $f=0.67$ , charge of  $-1.33$ ; P4,  $f=0.61$ , charge of  $-1.39$ ; P5,  $f=0.67$ , charge of  $-1.33$ ) are similar to those found for the soluble analogue Ins(1,3,4,5)P<sub>4</sub> [P3,  $f=0.64$ , charge of  $-1.36$ ; P4,  $f=0.56$ , charge of  $-1.44$ ; P5,  $f=0.71$ , charge of  $-1.29$  (data derived from ref 51)].

**Intermolecular versus Intramolecular Interactions.** For all phosphoinositides investigated in this study, the charges at pH 7.0 are approximately equal to or higher than the charges found for the respective phosphate groups of the corresponding soluble inositol polyphosphates (see above). The presence of negatively charged lipids in a bilayer increases the proton concentration at

Table 1:  $pK_{a2}$  Values and Charges for the Individual Phosphomonoesters of Phosphatidylinositol As Determined in This Study<sup>a</sup>

phosphoinositide	phosphate group position	$pK_{a2}$	charge (pH 7.0) ( $\pm 0.05$ )	overall charge (pH 7.0)
PI(3,5)P <sub>2</sub>	3	$6.96 \pm 0.04$	-1.52	$-4.25 \pm 0.10$
	5	$6.58 \pm 0.04$	-1.73	
PI(3,4)P <sub>2</sub>	3	not available	-1.48	$-3.96 \pm 0.10$
	4	not available	-1.48	
PI(4,5)P <sub>2</sub>	4	not available	-1.58	$-3.99 \pm 0.10$
	5	not available	-1.41	
PI(3,4,5)P <sub>3</sub>	3	not available	-1.33	$-5.05 \pm 0.15$
	4	not available	-1.39	
	5	not available	-1.33	

<sup>a</sup>The error indicated for the  $pK_{a2}$  values follows directly from the nonlinear curve fit, and the error in the total charge is an estimate which follows from the reproducibility in the  $f_{ip}$  determination and the reproducibility in the titration curve for PI(4,5)P<sub>2</sub> as shown in the Supporting Information. The error is a conservative estimate; i.e., the actual errors are likely to be lower.

the lipid–water interface, which results in a decreased intrinsic pH and, therefore, an increased apparent  $pK_a$  of the protonatable lipid group (58). On the basis of these simple electrostatic considerations, phosphoinositide lipids should be less charged

than the soluble inositol polyphosphate analogues for the same pH and ionic strength of the solution. The question why the opposite is observed in this case arises.

Kooijman et al. (42, 50) have recently shown for phosphatidic acid that intermolecular hydrogen bond formation (e.g., due to the presence of phosphatidylethanolamine or lysine- or arginine-rich peptides) leads to a reduced  $pK_{a2}$  and hence a higher charge of the phosphomonoester group. This suggests that the higher than expected charge at the phosphoinositide phosphomonoester groups might be due to the presence of a hydrogen bond donor molecule. Phosphatidylcholine, which is present as a matrix lipid in the mixed lipid vesicles used for the study reported here, cannot engage in hydrogen bond formation with the respective phosphoinositide. This leaves only mutual hydrogen bond formation between phosphoinositide molecules as a possible explanation for the higher than expected headgroup charge. Five types of hydrogen bonds can principally be formed in the headgroup moiety of phosphoinositides: phosphomonoester–phosphomonoester, phosphomonoester–hydroxyl, hydroxyl–hydroxyl, phosphomonoester–phosphodiester, and hydroxyl–phosphodiester. Hydrogen bonds involving the phosphodiester groups cannot be discussed here because the phosphodiester peak of the phosphoinositides cannot be distinguished from the significantly stronger phosphodiester peak associated with the PC component of the lipid mixture. Similarly, hydroxyl–hydroxyl group interactions cannot be probed with the current technique, and in addition, they are not expected to affect the  $pK_{a2}$  of the phosphomonoester groups.

Intermolecular sharing of a proton between phosphomonoester groups of adjacent phosphoinositide molecules appears to be unlikely. This can be best illustrated when the data obtained for PI(3,5)P<sub>2</sub> are analyzed. In that case, the pH-dependent chemical shift variation could be described by using eq 1. If the phosphomonoester groups of adjacent PI(3,5)P<sub>2</sub> molecules were sharing protons, a biphasic behavior of the pH-dependent chemical shift variation would be expected as observed for the intramolecular sharing of protons. In addition, a comparison of the pH-dependent chemical shift variation data obtained for PI(4,5)P<sub>2</sub> with the corresponding data reported in the literature for Ins(4,5)P<sub>2</sub> reveals a biphasic protonation behavior that has similar overall features. If the phosphomonoester groups in PI(4,5)P<sub>2</sub> were engaged in mutual intermolecular proton sharing, we would expect that the pH-dependent chemical shift variation would assume a form that is distinctively different from the behavior that is observed for Ins(4,5)P<sub>2</sub>.

This leaves only intermolecular hydroxyl–phosphomonoester group interactions as the probable cause for the observed increased charges of the phosphomonoester groups of phosphoinositide lipids. A comparison of the pH-dependent chemical shift values found for the phosphoinositide lipids with the corresponding values reported in the literature for inositol polyphosphates bears some risks due to the differing experimental conditions. However, it is striking that the phosphomonoester peaks of the phosphoinositides are found downfield from their counterparts observed for the soluble compounds [for example, the chemical shifts for Ins(4,5)P<sub>2</sub> at pH 4 are ~1.7 (P4) and ~1.2 (P5) (38)]. Such a downfield shift of the phosphomonoester peaks has previously been rationalized in general terms with an enhanced hydroxyl–phosphomonoester group interaction, resulting in an increased charge of the respective phosphomonoester group (39). Since the intramolecular hydrogen bond pattern is similar for the lipid headgroups and their soluble analogues, this enhanced

hydroxyl–phosphomonoester group interaction must have an intermolecular origin. The notion that phosphoinositide lipids show intermolecular interaction via hydrogen bond formation is surprising because the high headgroup charge was expected to give rise to strong repulsive forces. However, the hypothesis of an at least limited attractive mutual interaction is further supported by the fact that the chemical shifts of the respective phosphomonoester groups of PI(4,5)P<sub>2</sub> were largely unaffected by the phosphoinositide concentration in the lipid bilayer (1, 5, and 20%). If the phosphoinositide molecules were uniformly distributed in the lipid bilayer, increasing concentrations of PI(4,5)P<sub>2</sub> would change the surface charge density and, therefore, the environment of the respective PI(4,5)P<sub>2</sub> molecule, which should lead to a change in the <sup>31</sup>P chemical shift, as observed for phosphatidic acid (46). This is not the case here, and therefore, it appears that on the time scale of the NMR experiment, PI(4,5)P<sub>2</sub> is clustered at least to some extent. The notion of protein-independent PI(4,5)P<sub>2</sub> clustering has been introduced previously (59) and has been met with some skepticism (60–62). While it is outside the scope of this study to discuss this disagreement in detail, it is worth mentioning that in the latter studies phosphoinositides labeled with a bulky fluorescent group were the only phosphoinositide components present in the respective model system. In our previous studies (59, 63), we used unlabeled phosphoinositides mixed with small amounts of the corresponding fluorescently labeled phosphoinositide; i.e., in our case, the fluorescently labeled phosphoinositide molecule was a “reporter” of the phosphoinositide phase behavior rather than the only phosphoinositide component whose phase behavior is being investigated, which might explain the aforementioned disagreement. The notion of mutual PI(4,5)P<sub>2</sub> interaction has recently been further supported by Leventhal et al. (64, 65), who found that phosphoinositides form monolayers at the air–water interface that are significantly more condensed than expected on the basis of their high headgroup charge. In addition, computer simulation studies highlighted the possibility of formation of intermolecular hydrogen bonds between PI(4,5)P<sub>2</sub> headgroups (66, 67).

Our NMR study completely avoids the potential pitfalls associated with the use of fluorescently labeled phosphoinositides. Furthermore, this study links the results obtained for high PI(4,5)P<sub>2</sub> concentrations with the conditions found for physiological PI(4,5)P<sub>2</sub> concentrations (1 mol %). At present, the data can only be interpreted in terms of PI(4,5)P<sub>2</sub> clustering even at concentrations as low as 1 mol %. It appears that the high charge of the phosphoinositide headgroup is dissipated through intramolecular hydrogen bonding, resulting in a reduced charge density within the molecule. The local charge density is further reduced through formation of mutual hydrogen bonds between adjacent phosphoinositide molecules (directly or water mediated). The overall attractive forces are expected to be comparatively weak because repulsive electrostatic forces counterbalance the attractive forces due to hydrogen bond formation. Small changes in the molecular structure (e.g., the introduction of a bulky label in one of the acyl chains) might already offset this fine balance. Most importantly, environmental changes (e.g., the presence of other hydrogen donors) are expected to strongly affect the ionization behavior of phosphoinositides.

## CONCLUSIONS

This study shows that the ionization behavior of phosphoinositides is intimately linked to the positions of the phosphate

groups at the inositol ring of the phosphoinositide headgroup. Phosphoinositides form a complex intra- and intermolecular hydrogen bond network that leads to an intra- and intermolecular dissipation of the charges, which is most likely the reason for the weaker than expected repulsion between phosphoinositide molecules. Minor pH changes or changes in the overall environment of the lipids will have a pronounced effect on the hydrogen bond pattern and, therefore, the charge of the respective phosphoinositide headgroup. Therefore, it would be naive to believe that phosphoinositides will exhibit the same ionization properties as found in this study when embedded in the compositionally complex inner leaflet of the plasma membrane. Further studies involving more complex lipid mixtures are needed to explore the impact of other lipids on the ionization behavior of phosphoinositides and to address the question of whether PI(4,5)P<sub>2</sub> clusters when embedded in a complex lipid environment. Similarly, this study should be extended in the future to involve divalent cations and cationic proteins (peptides). First and foremost, the data obtained in this study highlight that mutual phosphoinositide interaction can be attractive rather than repulsive, while the question of whether PI(4,5)P<sub>2</sub> molecules are clustered in a biomembrane in vivo is important but not at the heart of this study. In physiological systems, the postulated attractive mutual interaction might be strong enough that PI(4,5)P<sub>2</sub> stays clustered for a sufficiently long time after it has been generated by kinases so that proteins can interact with the lipids to further stabilize locally enriched phosphoinositide domains. Another important finding of this study is that the ionization behavior of the phosphoinositide derivatives differs, which might be an important aspect for the selective targeting of proteins to specific membrane environments.

## ACKNOWLEDGMENT

We acknowledge Satyen Kumar, Michael Brown, and Avigdor Leftin for insightful discussions and Satyen Kumar for a careful reading of the manuscript.

## SUPPORTING INFORMATION AVAILABLE

A discussion about the static NMR spectra, includes a discussion about the formation of metastable states for certain sample preparation procedures and presents <sup>31</sup>P NMR MAS data for PI(4,5)P<sub>2</sub> as a function of concentration. These Supporting Information may be accessed free of charge online at <http://pubs.acs.org>. This material is available free of charge via the Internet at <http://pubs.acs.org>.

## REFERENCES

- Lemmon, M. A. (2003) Phosphoinositide recognition domains. *Traffic* 4, 201–213.
- Lemmon, M. A. (2008) Membrane recognition by phospholipid-binding domains. *Nat. Rev. Mol. Cell Biol.* 9, 99–111.
- Rusten, T. E., and Stenmark, H. (2006) Analyzing phosphoinositides and their interacting proteins. *Nat. Methods* 3, 251–258.
- Janetopoulos, C., and Devreotes, P. (2006) Phosphoinositide signaling plays a key role in cytokinesis. *J. Cell Biol.* 174, 485–490.
- McLaughlin, S., and Murray, D. (2005) Plasma membrane phosphoinositide organization by protein electrostatics. *Nature* 438, 605–611.
- Mao, Y. S., and Yin, H. L. (2007) Regulation of the actin cytoskeleton by phosphatidylinositol 4-phosphate 5 kinases. *Pfluegers Arch.* 455, 5–18.
- Kockskamper, J., Zima, A. V., Roderick, H. L., Pieske, B., Blatter, L. A., and Bootman, M. D. (2008) Emerging roles of inositol 1,4,5-trisphosphate signaling in cardiac myocytes. *J. Mol. Cell. Cardiol.* 45, 128–147.
- Merida, I., Avila-Flores, A., and Merino, E. (2008) Diacylglycerol kinases: At the hub of cell signalling. *Biochem. J.* 409, 1–18.
- Suh, P. G., Park, J. I., Manzoli, L., Cocco, L., Peak, J. C., Katan, M., Fukami, K., Kataoka, T., Yun, S., and Ryu, S. H. (2008) Multiple roles of phosphoinositide-specific phospholipase C isozymes. *BMB Rep.* 41, 415–434.
- Astle, M. V., Horan, K. A., Ooms, L. M., and Mitchell, C. A. (2007) The inositol polyphosphate 5-phosphatases: Traffic controllers, waistline watchers and tumour suppressors? In *Cell Biology of Inositol Lipids and Phosphates*, pp 161–181.
- Hilgemann, D. W. (2007) Local PIP<sub>2</sub> signals: When, where, and how? *Pfluegers Arch.* 455, 55–67.
- Yin, H. L., and Janmey, P. A. (2003) Phosphoinositide regulation of the actin cytoskeleton. *Annu. Rev. Physiol.* 65, 761–789.
- Suh, B. C., and Hille, B. (2008) PIP<sub>2</sub> is a necessary cofactor for ion channel function: How and why? *Annu. Rev. Biophys.* 37, 175–195.
- Lindmo, K., and Stenmark, H. (2006) Regulation of membrane traffic by phosphoinositide 3-kinases. *J. Cell Sci.* 119, 605–614.
- Shaw, R. J., and Cantley, L. C. (2006) Ras, PI(3)K and mTOR signalling controls tumour cell growth. *Nature* 441, 424–430.
- Taniguchi, C. M., Emanuelli, B., and Kahn, C. R. (2006) Critical nodes in signalling pathways: Insights into insulin action. *Nat. Rev. Mol. Cell Biol.* 7, 85–96.
- Keniry, M., and Parsons, R. (2008) The role of PTEN signaling perturbations in cancer and in targeted therapy. *Oncogene* 27, 5477–5485.
- Vogt, P. K., Kang, S., Eislinger, M. A., and Gymnopoulos, M. (2007) Cancer-specific mutations in phosphatidylinositol 3-kinase. *Trends Biochem. Sci.* 32, 342–349.
- Gericke, A., Munson, M., and Ross, A. H. (2006) Regulation of PTEN phosphatase. *Gene* 374, 1–9.
- Backers, K., Blero, D., Paternotte, N., Zhang, J., and Erneux, C. (2003) The termination of PI3K signalling by SHIP1 and SHIP2 inositol 5-phosphatases. *Adv. Enzyme Regul.* 43, 15–28.
- Vanhaesebroeck, B., Leever, S. J., Ahmadi, K., Timms, J., Katso, R., Driscoll, P. C., Woscholski, R., Parker, P. J., and Waterfield, M. D. (2001) Synthesis and function of 3-phosphorylated inositol lipids. *Annu. Rev. Biochem.* 70, 535–602.
- Ma, K., Cheung, S. M., Marshall, A. J., and Duronio, V. (2008) PI(3,4,5)P<sub>3</sub> and PI(3,4)P<sub>2</sub> levels correlate with PKB/akt phosphorylation at Thr308 and Ser473, respectively: PI(3,4)P<sub>2</sub> levels determine PKB activity. *Cell. Signalling* 20, 684–694.
- Nystuen, A., Legare, M. E., Shultz, L. D., and Frankel, W. N. (2001) A null mutation in inositol polyphosphate 4-phosphatase type I causes selective neuronal loss in weble mutant mice. *Neuron* 32, 203–212.
- Shin, H. W., Hayashi, M., Christoforidis, S., Lacas-Gervais, S., Hoepfner, S., Wenk, M. R., Modregger, J., Uttenweiler-Joseph, S., Wilm, M., Nystuen, A., Frankel, W. N., Solimena, M., De Camilli, P., and Zerial, M. (2005) An enzymatic cascade of Rab5 effectors regulates phosphoinositide turnover in the endocytic pathway. *J. Cell Biol.* 170, 607–618.
- Dowler, S., Currie, R. A., Campbell, D. G., Deak, M., Kular, G., Downes, C. P., and Alessi, D. R. (2000) Identification of pleckstrin-homology-domain-containing proteins with novel phosphoinositide-binding specificities. *Biochem. J.* 351, 19–31.
- Krause, M., Leslie, J. D., Stewart, M., Lafuente, E. M., Valderrama, F., Jagannathan, R., Strasser, G. A., Robinson, D. A., Liu, H., Way, M., Yaffe, M. B., Boussiotis, V. A., and Gertler, F. B. (2004) Lamellipodin, an Ena/NASP ligand, is implicated in the regulation of lamellipodial dynamics. *Dev. Cell* 7, 571–583.
- Michell, R. H., Heath, V. L., Lemmon, M. A., and Dove, S. K. (2006) Phosphatidylinositol 3,5-bisphosphate: Metabolism and cellular functions. *Trends Biochem. Sci.* 31, 52–63.
- Ikonomov, O. C., Sbrissa, D., and Shisheva, A. (2006) Localized PtdIns 3,5-P<sub>2</sub> synthesis to regulate early endosome dynamics and. *Am. J. Physiol.* 291, C393–C404.
- Jefferies, H. B. J., Cooke, F. T., Jat, P., Boucheron, C., Koizumi, T., Hayakawa, M., Kaizawa, H., Ohishi, T., Workman, P., Waterfield, M. D., and Parker, P. J. (2008) A selective PIKfyve inhibitor blocks PtdIns(3,5) P<sub>2</sub> production and disrupts endomembrane transport and retroviral budding. *EMBO Rep.* 9, 164–170.
- Cabezas, A., Pattani, K., and Stenmark, H. (2006) Cloning and subcellular localization of a human phosphatidylinositol 3-phosphate 5-kinase, PIKfyve/Fab1. *Gene* 371, 34–41.
- Rutherford, A. C., Traer, C., Wassmer, T., Pattani, K., Bujny, M. V., Carlton, J. G., Stenmark, H., and Cullen, P. J. (2006) The mammalian phosphatidylinositol 3-phosphate 5-kinase (PIKfyve) regulates endosome-to-TGN retrograde transport. *J. Cell Sci.* 119, 3944–3957.



32. Sbrissa, D., Ikononov, O. C., Fu, Z. Y., Ijuin, T., Gruenberg, J., Takenawa, T., and Shisheva, A. (2007) Core protein machinery for mammalian phosphatidylinositol 3,5-bisphosphate synthesis and turnover that regulates the progression of endosomal transport: Novel sac phosphatase joins the arpkfyve-pikfyve complex. *J. Biol. Chem.* 282, 23878–23891.
33. Blero, D., Payraastre, B., Schurmans, S., and Erneux, C. (2007) Phosphoinositide phosphatases in a network of signalling reactions. *Pfluegers Arch.* 455, 31–44.
34. Zhang, Y., Zolov, S. N., Chow, C. Y., Slutsky, S. G., Richardson, S. C., Piper, R. C., Yang, B., Nau, J. J., Westric, R. J., Morrison, S. J., Meisler, M. H., and Weisman, L. S. (2007) Loss of Vac14, a regulator of the signaling lipid phosphatidylinositol 3,5-bisphosphate, results in neurodegeneration in mice. *Proc. Natl. Acad. Sci. U.S.A.* 104, 17518–17523.
35. Nicot, A. S., and Laporte, J. (2008) Endosomal phosphoinositides and human diseases. *Traffic* 9, 1240–1249.
36. van Paridon, P. A., de Kruijff, B., Ouwerkerk, R., and Wirtz, K. W. A. (1986) Polyphosphoinositides undergo charge neutralization in the physiological pH range: A  $^{31}\text{P}$ -NMR study. *Biochim. Biophys. Acta* 877, 216–219.
37. Schlewer, G., Guedat, P., Ballereau, S., Schmitt, L., Spiess, B. (1998) Inositol Phosphates: Intramolecular physico-chemical studies: Correlation with binding properties. In *Phosphoinositides: Chemistry, Biochemistry and Biomedical Applications* (Bruzik, K. S., Ed.) pp 255–270, American Chemical Society, Washington, DC.
38. Schmitt, L., Bortmann, P., Schlewer, G., and Spiess, B. (1993) Myoinositol 1,4,5-triphosphate and related compounds protonation sequence: Potentiometric and P-31 studies. *J. Chem. Soc., Perkin Trans. 2*, 2257–2263.
39. Ballereau, S., Guedat, P., Poirier, S. N., Guillemette, G., Spiess, B., and Schlewer, G. (1999) Synthesis, acid-base behavior, and binding properties of 6-modified myo-inositol 1,4,5-tris(phosphate)s. *J. Med. Chem.* 42, 4824–4835.
40. Felemez, M., Bernard, P., Schlewer, G., and Spiess, B. (2000) Intramolecular protonation process of myo-inositol 1,4,5-tris(phosphate) and related compounds: Dynamics of the intramolecular interactions and evidence of C-H...O hydrogen bonding. *J. Am. Chem. Soc.* 122, 3156–3165.
41. Felemez, M., and Spiess, B. (2003) H-1 NMR titrations of hydroxy protons in aqueous solution as a method of investigation of intramolecular hydrogen-bonding in phosphorylated compounds: Examples of myo-inositol 2-phosphate and myo-inositol 1,2,6-tris(phosphates). *J. Am. Chem. Soc.* 125, 7768–7769.
42. Kooijman, E. E., Carter, K. M., van Laar, E. G., Chupin, V., Burger, K. N. J., and de Kruijff, B. (2005) What makes the bioactive lipids phosphatidic acid and lysophosphatidic acid so special? *Biochemistry* 44, 17007–17015.
43. Appleton, T. G., Hall, J. R., Ralph, S. F., and Thompson, C. S. M. (1989) NMR study of acid-base equilibria and other reactions of ammineplatinum complexes with aqua and hydroxo ligands. *Inorg. Chem.* 28, 1989–1993.
44. Koter, M., de Kruijff, B., and van Deenen, L. L. (1978) Calcium-induced aggregation and fusion of mixed phosphatidylcholine-phosphatidic acid vesicles as studied by  $^{31}\text{P}$  NMR. *Biochim. Biophys. Acta* 514, 255–263.
45. Hauser, H. (1989) Mechanism of spontaneous vesiculation. *Proc. Natl. Acad. Sci. U.S.A.* 86, 5351–5355.
46. Swairjo, M. A., Seaton, B. A., and Roberts, M. F. (1994) Effect of vesicle composition and curvature on the dissociation of phosphatidic acid in small unilamellar vesicles: A  $^{31}\text{P}$  NMR study. *Biochim. Biophys. Acta* 1191, 354–361.
47. Kooijman, E. E., Sot, J., Montes, L. R., Alonso, A., Gericke, A., de Kruijff, B., Kumar, S., and Goni, F. M. (2008) Membrane organization and ionization behavior of the minor but crucial lipid ceramide-1-phosphate. *Biophys. J.* 94, 4320–4330.
48. Watts, A. (1998) Solid-state NMR approaches for studying the interaction of peptides and proteins with membranes. *Biochim. Biophys. Acta* 1376, 297–318.
49. Traikia, M., Warschawski, D. E., Lambert, O., Rigaud, J. L., and Devaux, P. F. (2002) Asymmetrical membranes and surface tension. *Biophys. J.* 83, 1443–1454.
50. Kooijman, E. E., Tieleman, D. P., Testerink, C., Munnik, T., Rijkers, D. T. S., Burger, K. N. J., and de Kruijff, B. (2007) An electrostatic/hydrogen bond switch as the basis for the specific interaction of phosphatidic acid with proteins. *J. Biol. Chem.* 282, 11356–11364.
51. Guedat, P., Schlewer, G., Krempp, E., Riley, A. M., Potter, B. V. L., and Spiess, B. (1997) Investigation of the intramolecular acid-base properties of D-myo-inositol 1,3,4,5-tetrakisphosphate and DL-myo-inositol 1,2,4,5-tetrakisphosphate. *Chem. Commun.*, 625–626.
52. Schmitt, L., Bortmann, P., Spiess, B., and Schlewer, G. (1993) Synthesis, potentiometric and P-31-NMR investigations of the ionization state and complexation properties of inositol phosphates: Biological consequences. *Phosphorus, Sulfur Silicon Relat. Elem.* 76, 407–410.
53. Cullis, P. R., and Dekruiff, B. (1979) Lipid Polymorphism and the Functional Roles of Lipids in Biological-Membranes. *Biochim. Biophys. Acta* 559, 399–420.
54. Kooijman, E. E., Chupin, V., Fuller, N. L., Kozlov, M. M., de Kruijff, B., Burger, K. N. J., and Rand, P. R. (2005) Spontaneous curvature of phosphatidic acid and lysophosphatidic acid. *Biochemistry* 44, 2097–2102.
55. Horne, G., Maechling, C., Fleig, A., Hirata, M., Penner, R., Spiess, B., and Potter, B. V. L. (2004) D-6-Deoxy-myo-inositol 1,3,4,5-tetrakisphosphate, a mimic of D-myo-inositol 1,3,4,5-tetrakisphosphate: Biological activity and pH-dependent conformational properties. *Biochem. Biophys. Res. Commun.* 320, 1262–1270.
56. Borkovec, M., and Spiess, B. (2004) Microscopic ionization mechanism of inositol tetrakisphosphates. *Phys. Chem. Chem. Phys.* 6, 1144–1151.
57. Schmitt, L., Spiess, B., and Schlewer, G. (1995) Synthesis and binding properties of myoinositol 4,5,6-tris(phosphate), an analog of myoinositol 1,4,5-tris(phosphate): Correlation with the ionization state of the molecules. *Bioorg. Med. Chem. Lett.* 5, 1225–1230.
58. Cevc, G. (1990) Membrane Electrostatics. *Biochim. Biophys. Acta* 1031, 311–382.
59. Redfern, D. A., and Gericke, A. (2005) pH dependent microdomain formation in phosphatidylinositol polyphosphate/phosphatidylcholine mixed vesicles. *J. Lipid Res.* 46, 504–515.
60. Blin, G., Margeat, E., Carvalho, K., Royer, C. A., Roy, C., and Picart, C. (2008) Quantitative analysis of the binding of ezrin to large unilamellar vesicles containing phosphatidylinositol 4,5-bisphosphate. *Biophys. J.* 94, 1021–1033.
61. Fernandes, F., Loura, L. M. S., Fedorov, A., and Prieto, M. (2006) Absence of clustering of phosphatidylinositol-(4,5)-bisphosphate in fluid phosphatidylcholine. *J. Lipid Res.* 47, 1521–1525.
62. Gamper, N., and Shapiro, M. S. (2007) Target-specific PIP2 signalling: How might it work? *J. Physiol. (Oxford, U.K.)* 582, 967–975.
63. Redfern, D. A., and Gericke, A. (2004) Domain formation in phosphatidylinositol monophosphate/phosphatidylcholine model membrane systems. *Biophys. J.* 86, 2980–2992.
64. Levental, I., Cebers, A., and Janmey, P. A. (2008) Combined electrostatics and hydrogen bonding determine intermolecular interactions between polyphosphoinositides. *J. Am. Chem. Soc.* 130, 9025–9030.
65. Levental, I., Janmey, P. A., and Cebers, A. (2008) Electrostatic contribution to the surface pressure of charged monolayers containing polyphosphoinositides. *Biophys. J.* 95, 1199–1205.
66. Liepina, I., Czaplowski, C., Janmey, P., and Liwo, A. (2003) Molecular dynamics study of a gelsolin-derived peptide binding to a lipid bilayer containing phosphatidylinositol 4,5-bisphosphate. *Biopolymers* 71, 49–70.
67. Lorenz, C. D., Faraudo, J., and Travesset, A. (2008) Hydrogen bonding and binding of polybasic residues with negatively charged mixed lipid monolayers. *Langmuir* 24, 1654–1658.